

The Enskog–Vlasov equation: A kinetic model describing gas, liquid, and solid

E. S. Benilov* and M. S. Benilov†

(Dated: September 10, 2022)

The Enskog–Vlasov (EV) equation is a widely used semiempiric kinetic model of gas-liquid phase transitions. These are described by an instability with respect to infinitely long perturbations, developing in a gas state when the temperature drops below (or density rises above) a certain threshold. In this paper, we show that the EV equation describes one more instability, with respect to perturbations with a finite wavelength and occurring at a higher density. This instability corresponds to fluid-solid phase transition and the perturbations’ wavelength is essentially the characteristic scale of the emerging crystal structure. Thus, even though the EV model does not describe the fundamental physics of the solid state, it can ‘mimic’ it – and, thus, can be used in applications involving both evaporation and solidification of liquids. Our results also predict to which extent a pure fluid can be overcooled before it definitely turns into a solid.

INTRODUCTION

The Enskog–Vlasov (EV) kinetic equation comprises the Enskog collision integral for dense fluids [1] and a Vlasov term describing the van-der-Waals force. The first version of the EV model [2, 3] was based on the original form of the Enskog integral – which, as shown in Ref. [4], does not comply with the Onsager relations. Ref. [4] also proposed a modification of the Enskog integral free from this shortcoming, and it was incorporated in the EV model in Refs. [5, 6]. Refs. [7–9] showed that an H-theorem holds for the EV equation only subject to a certain restriction of its coefficients, and Ref. [10] proposed a version of the EV equation that satisfies it and conserves energy as well (all of the previous versions do not).

Note that, in kinetic models, phase transitions correspond to instabilities. For the original version of the EV equation, the presence of an instability has been shown in Ref. [3], and it was interpreted as gas-liquid phase transition.

In the present paper, we report the results of a more detailed study. Using the EV equation that conserves energy and satisfies an H-theorem, we find *two* different instabilities, with respect to infinite- and finite-wavelength perturbations – interpreted as gas-liquid and fluid-solid transitions, respectively. The latter result comes as a surprise, as the EV equation was conceived as a tool for modeling of fluids only. We show, however, that it admits periodic solutions capable of ‘mimicking’ the solid phase.

THE ENSKOG–VLASOV MODEL

The EV model assumes the following parameters as given: the molecule’s effective diameter D , the Vlasov

potential $\Phi(r)$ characterizing the van der Waals attraction of two molecules separated by a distance r , and the functional $Q[n]$ depending on the number density $n(\mathbf{r})$ and representing the non-ideal part of the entropy. Note that, within the framework of the EV model, $Q[n]$ does not depend on the temperature T .

The main characteristic of $\Phi(r)$ (one that affects the fluid’s macroscopic properties) is

$$E = - \int \Phi(r) d^3\mathbf{r}, \quad (1)$$

which suggest the following nondimensional variables:

$$\begin{aligned} \Phi_{nd} &= \frac{\Phi}{ED^3}, & Q_{nd} &= \frac{Q}{k_B}, & (2) \\ \mathbf{r}_{nd} &= \frac{\mathbf{r}}{D}, & n_{nd} &= D^3 n, & T_{nd} &= \frac{k_B}{ED^3} T, & (3) \end{aligned}$$

where k_B is the Boltzmann constant. Note that, due to (1), the nondimensional Vlasov potential Φ_{nd} satisfies (the subscript $_{nd}$ omitted)

$$\int \Phi(r) d^3\mathbf{r} = -1. \quad (4)$$

We also assume that $\Phi(r)$ is a monotonically growing function of r , i.e., the van der Waals force is attractive everywhere. Together with the requirement that the integral in (4) converge, this amounts to the condition $\Phi(r) < 0$ for all r .

Refs. [7–9] showed that the EV equation satisfies an H-theorem only if $Q[n]$ satisfies a certain constraint, with Ref. [10] presenting a wide class of $Q[n]$ that do. In terms of variables (2)–(3) (subscripts $_{nd}$ omitted), this class is

$$Q[n] = -\frac{1}{2} \int \int n(\mathbf{r}) n(\mathbf{r}_1) H(1 - |\mathbf{r} - \mathbf{r}_1|) d^3\mathbf{r} d^3\mathbf{r}_1 - \sum_{l=2}^{\infty} \frac{c_l}{l(l+1)} \int \int n(\mathbf{r}) \left[\prod_{i=1}^l n(\mathbf{r}_i) H(1 - |\mathbf{r} - \mathbf{r}_i|) \right] \left[\prod_{i=1}^{l-1} \prod_{j=i+1}^l H(1 - |\mathbf{r}_i - \mathbf{r}_j|) \right] d^3\mathbf{r} \prod_{i=1}^l d^3\mathbf{r}_i, \quad (5)$$

where H is the Heaviside function, \int^l denotes l repeated integrals, and $c_2, c_3, c_4 \dots$ are constants specific to the fluid, or the group of fluids, under consideration (note that there is no c_1).

We also introduce a function $\Theta(n)$ related to the functional $Q[n]$ by

$$\frac{1}{n} [n\Theta(n)]' = - \left. \frac{\delta\Theta[n]}{\delta n(\mathbf{r})} \right|_{n=\text{const}},$$

where $'$ denotes differentiation with respect to n . Taking into account (5), we obtain

$$\Theta(n) = \frac{2\pi}{3} n + \sum_{l=2}^{\infty} \frac{c_l A_l}{l(l+1)} n^l, \quad (6)$$

where

$$A_l = \int \left[\prod_{i=1}^l H(1 - |\mathbf{r}_i|) \right] \times \left[\prod_{i=1}^{l-1} \prod_{j=i+1}^l H(1 - |\mathbf{r}_i - \mathbf{r}_j|) \right] \prod_{i=1}^l d^3\mathbf{r}_i \quad (7)$$

are numeric constants. $\Theta(n)$ plays an important role in the thermodynamics of EV fluids [10]: in particular, their nondimensional equation of state (EoS) is

$$p = nT [1 + n\Theta'(n)] - \frac{1}{2} n^2. \quad (8)$$

THE ANALYSIS

To examine the stability of equilibrium solutions of the EV equation, we seek linear harmonic perturbations with zero frequency (frozen waves). They are excellent stability indicators: if a frozen wave with a wavenumber k exists for a certain state, one can be sure that either a small increase or a small decrease of k would make it unstable. Thus, the parameter values for which the first frozen wave bifurcates from the base state corresponds to the onset of instability.

Searching for frozen waves requires only the steady-state version of the EV equation, which – unlike steady-state versions of other kinetic models – does not include the velocity of molecules [3] and is, thus, relatively simple.

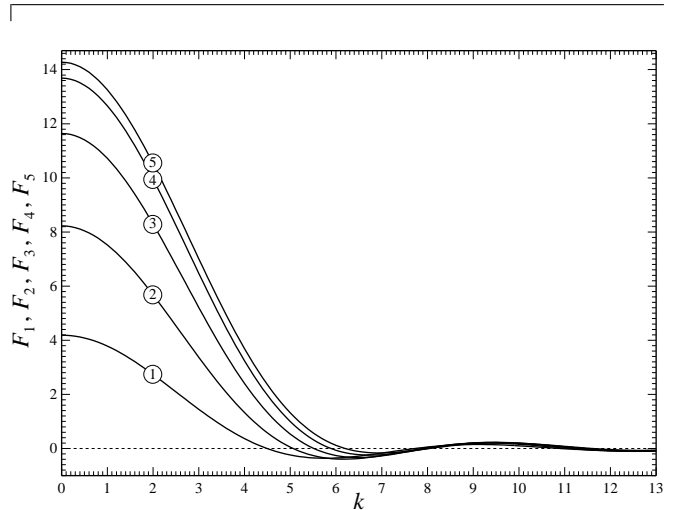


FIG. 1. The functions $F_l(k)$ defined by (11). The curves are marked with the corresponding value of l .

The equilibrium version of the EV equation [see Ref. [10], Eq. (30)] is

$$\ln n(\mathbf{r}) + \frac{1}{\bar{T}} \int n(\mathbf{r}_1) \Phi(|\mathbf{r} - \mathbf{r}_1|) d^3\mathbf{r}_1 - \frac{\delta Q[n]}{\delta n(\mathbf{r})} = \text{const}, \quad (9)$$

where \bar{T} is the temperature of the (spatially uniform) base state under consideration. Replacing $Q[n]$ with series (5) and setting $n(\mathbf{r}) = \bar{n} + \tilde{n}(\mathbf{r})$ where \bar{n} is the density of the base state and $\tilde{n}(\mathbf{r})$ is a small perturbation, we linearize Eq. (9). Letting $\tilde{n}(\mathbf{r}) = e^{ikz}$, where k is the wavenumber and z is one of the spatial coordinates, we obtain (overbars omitted)

$$T = - \frac{n\hat{\Phi}(k)}{1 + nF_1(k) + \sum_{l=2}^{\infty} c_l n^l F_l(k)}, \quad (10)$$

where

$$F_l(k) = \int \left[\prod_{j=1}^l H(1 - |\mathbf{r}_j|) \right] \times \left[\prod_{j=1}^{l-1} \prod_{i=j+1}^l H(1 - |\mathbf{r}_j - \mathbf{r}_i|) \right] \cos kz_l \prod_{j=1}^l d^3\mathbf{r}_j, \quad (11)$$

$$\hat{\Phi}(k) = \int \Phi(|\mathbf{r}|) \cos kz d^3\mathbf{r}.$$

Note that, due to constraint (4),

$$\hat{\Phi}(0) = -1. \quad (12)$$

Functions $F_l(k)$ do not involve any parameters. The first two can be calculated analytically, and another three have been computed using the Monte-Carlo method. All five are depicted in Fig. 1.

Equality (10) is, essentially, an instability criterion: if a value of k exists such that (10) is satisfied for a state (n, T) , this state is unstable.

THE RESULTS

In what follows, we shall illustrate criterion (10) using the values for the coefficients c_l , obtained in Ref. [11] for noble gases,

$$c_2 = -1.3207, \quad c_3 = 9.9308, \quad (13)$$

$$c_4 = -18.7526, \quad c_5 = 13.1406, \quad (14)$$

$$c_l = 0 \quad \text{for} \quad l \geq 6. \quad (15)$$

As seen later, the shape of the Vlasov potential is of little importance, so we assume, on a more or less ad hoc basis,

$$\hat{\Phi}(k) = -\frac{1}{1 + (Rk)^4}, \quad (16)$$

where R is, physically, the ratio of the spatial scale of the van der Waals force to the molecule's size. Evidently, expression (16) complies with restriction (12).

The stability criterion (10), (13)-(16) describes a one-parameter family of curves $T = T(n)$ with k being the parameter. The behavior of these curves depends on whether or not the fifth-order polynomial in n in the denominator of expression (10) has positive roots. Computations show that no more than one such root exists, and it (dis)appear only if $F_5(k)$ changes sign – which it does indeed do for infinite sequence of values of k tending towards infinity. Denoting these values by k_1, k_2, k_3, \dots , we have computed

$$k_1 \approx 6.2042, \quad k_2 \approx 8.0354, \quad k_3 \approx 11.6014.$$

It can also be verified by a straightforward analysis of expression (10) that, in the range

$$0 < k < k_1, \quad (17)$$

the denominator of expression (10) does *not* have positive roots. As a result – and due to quick decay of $\hat{\Phi}(k)$ as k increases – the curves $T(n)$ ‘recede’ within range (17) – see Fig. 2. Thus, the curve with $k = 0$ determines the boundary of an instability region, which will be referred to as IR1.

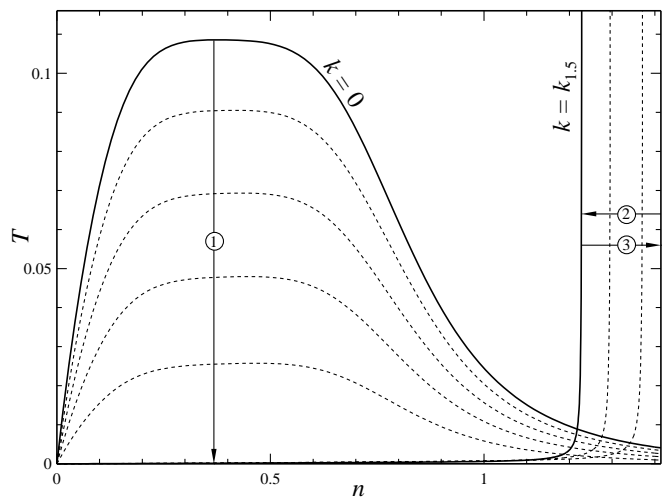


FIG. 2. Existence of frozen waves on the (n, T) plane. The curves $T(n)$ are determined by (10), (13)-(16) with $R = 1$. Dotted curves within ranges (1)-(3) correspond to k being within ranges (17)-(19), respectively. The boundaries of the instability regions are shown by solid lines.

Another instability region (IR2) arises for the range $k_1 < k < k_2$ – which can be conveniently subdivided into two subranges,

$$k_1 < k < k_{1.5}, \quad (18)$$

with $k_{1.5} \approx 7.129$, and

$$k_{1.5} < k < k_2. \quad (19)$$

As k changes from k_1 to $k_{1.5}$, the (real positive) root n_0 of the denominator of (10) ‘travels’ from $+\infty$ to $n_0 \approx 1.230$ – and when k changes from $k_{1.5}$ to k_2 , n_0 travels back to $+\infty$. Thus, the boundary of IR2 corresponds to $k = k_{1.5}$; the corresponding curve $T(n)$ is shown in Fig. 2 together with examples of curves for k from ranges (18) and (19).

A basic analysis of expression (10) and computations show that the instability regions corresponding to (k_2, k_3) , (k_3, k_4) , etc. are all *inside* IR1 and IR2 and, thus, are physically unimportant.

Finally, if $n \ll 1$ (diluted gas), the stability criterion (10) agrees with the corresponding results obtained in Refs. [12, 13] for the BGK–Vlasov and Boltzmann–Vlasov models, respectively.

DISCUSSION

For $k = 0$ (the boundary of IR1), (10) and (12) reduce to

$$T = \frac{n}{1 + \frac{4\pi}{3} n A_1 + \sum_{l=2}^{\infty} c_l n^l A_l},$$

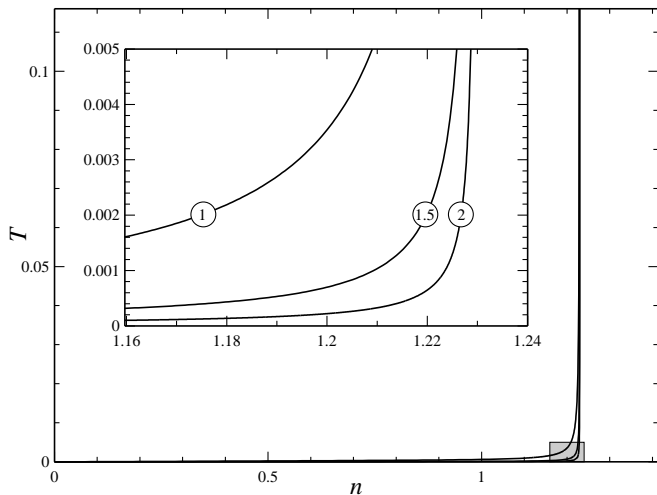


FIG. 3. The dependence of the boundary of IR2 on the parameter R of the Fourier transform (16) of the Vlasov potential. The inset shows a blow-up of the shaded region of the main panel. The curves are marked with the corresponding values of R .

where constants A_l are given by (7). The above expression can be rewritten in terms of the function $\Theta(n)$ [see (6)],

$$T = \frac{n}{1 + [n^2\Theta'(n)]'}. \quad (20)$$

This representation of the boundary of IR1 turns out to be very useful.

(1) Eq. (20) implies that IR1 does not depend on the specific shape of the Vlasov potential Φ .

(2) As for IR2, it does depend on Φ , but this dependence is weak – which we illustrate by computing the boundary of IR2 for different values of the parameter R [which appears in expression (16)] and plotting the results in Fig. 3. One can see that, for $R \gtrsim 2$, the boundary of IR2 is virtually indistinguishable from a vertical line. This effect is even more pronounced if $\hat{\Phi}(k)$ decays exponentially with k .

Given that the van der Waals force is supposed to be long-range (by comparison with the molecule size), one can assume that $R \gg 1$, and thus replace the boundary of IR2 by a vertical line. Physically, this means that a fluid cannot be compressed beyond a certain density value.

(3) Using EoS (8), one can show that the maximum of the function $T(n)$ given by (20) corresponds to the critical point.

(4) Not all of the stable states are physically meaningful, as some of them correspond to negative pressure. These can be detected using EoS (8). For the case (13)-(16) with $R = 1$, the full diagram of stable and physically meaningful fluid states is shown in Fig. 4.

(5) As stated in most thermodynamics texts, a non-

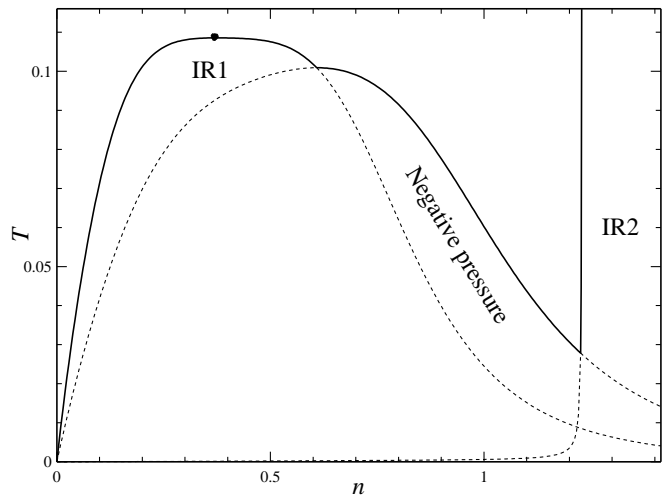


FIG. 4. The stable, physically meaningful fluid states in the (n, T) parameter plane. IR1 and IR2 stand for instability regions 1 and 2, respectively. The black dot marks the critical point.

ideal gas becomes unstable if

$$\left(\frac{\partial p}{\partial n}\right)_{T=\text{const}} < 0, \quad (21)$$

i.e., if an increase of density gives rise to a decrease of pressure. Applying this argument to EoS (8), we recover Eq. (20) describing the boundary of IR1.

IR2, in turn, is located in high-density region – hence, it may only describe fluid-solid transitions. Most importantly, the whole boundary of IR2 corresponds to a single value of the perturbation wavenumber, $k_{1.5}$ – so that $2\pi/k_{1.5}$ can be identified with the spatial scale of the emerging crystal. This agrees with the fact that that crystal structure does not depend on the temperature or density of the state where the transition takes place.

(6) It is well-known that gas-liquid phase transition typically occurs *before* criterion (21) predicts it. The threshold where the actual transition occurs is determined by the so-called evaporation curve describing the gas-liquid equilibrium. It is still possible, however, to overcool a gas or overheat a liquid beyond this threshold, provided they are sufficiently pure. Thus, the boundaries of the instability regions are essentially the limits to which one can overcool or overheat a fluid before phase transition occurs.

To illustrate this interpretation, we have redrawn Fig. 4 on the (T, p) plane, thus turning it into a *phase diagram* – see Fig. 5. We have also added empirically-derived evaporation, melting, and sublimation curves (the last two describe the solid-liquid and solid-gas equilibria, respectively).

The following features of Fig. 5 can be observed:

- There are two single-phase regions: in the one marked “S”, only solid phase exists – and in the

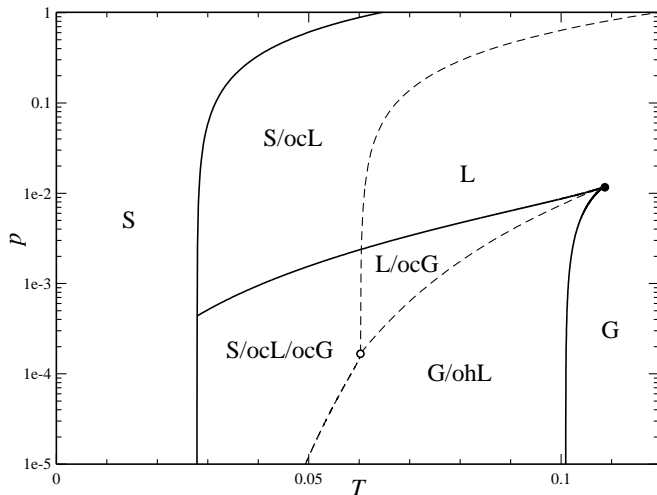


FIG. 5. The phase diagram for argon in the nondimensional (T, p) plane. Solid lines correspond to the boundaries of the instability regions computed using the EV model; dashed lines show the empiric evaporation, melting, and sublimation curves [14]. The critical and triple points are marked by a black dot and small circle, respectively. “G”, “L”, and “S” mark the regions where gas, liquid, and solid may exist; the prefixes “oc” and “oh” mean “overcooled” and “overheated”.

one whose parts are marked “L” or “G”, one of the two fluid phases exists (gas and liquid are difficult to separate in the latter case, as they can be continuously transformed one into another).

- In the transitional zone marked “S/ocL”, either solid or overcooled liquid can exist – and in the zone “S/ocL/ocG”, it is either solid or overcooled liquid, or overcooled gas.
- In the remaining two zones, “L/ocG” and “G/ohL”, either of the two fluid phases can exist.

CONCLUDING REMARKS

In this work, we have used the Enskog–Vlasov model to examine when fluids are unstable, and with respect to which perturbations. The parameter range of the instability is illustrated in Fig. 4 on the nondimensional (n, T) plane, and in Fig. 5, on the (T, p) plane. These figures are the main results of this work.

Note that, in Fig. 5, we have calculated only the solid curves, whereas the dashed ones have been obtained by methods of statistical thermodynamics [14]. This does not mean that the EV model cannot be used to calculate the latter: in fact, it *has* been used for calculating the evaporation curve, producing a result with an error

of only several percent [11]. Before calculating the melting and sublimation curves, however, one should explore periodic solutions of the EV equation which describe the solid (crystal) state; these solutions bifurcate from the spatially uniform (fluid) solutions as frozen waves. That is, we do not claim that the EV model can describe the fundamental physics of the solid state – but we do hope that it can ‘mimic’ it given a suitable choice of the functional $Q[n]$ and the Vlasov potential Φ . In fact, the Enskog approach to dense fluids has indeed been successfully used for description of hard-sphere crystals [15, 16].

Once the EV model is calibrated to deal with all three phases, it would become an invaluable tool for modeling complex physical problems (e.g., evolution of liquid films with evaporation and solidification).

The authors acknowledge the support of the Science Foundation Ireland through grant 12/IA/1683, and Fundação para a Ciência e a Tecnologia of Portugal through project Pest-OE/UID/FIS/50010/2013.

* Department of Mathematics and Statistics, University of Limerick, V94 T9PX, Ireland; Eugene.Benilov@ul.ie; <http://www.staff.ul.ie/eugenebenilov/hpage/>

† Departamento de Física, CCCEE, Universidade da Madeira, Largo do Município, 9000 Funchal, Portugal; Instituto de Plasmas e Fusão Nuclear, Instituto Superior Técnico, Universidade de Lisboa, Portugal; benilov@uma.pt; <http://fisica.uma.pt/ingles/pessoal/MikhailBenilov/>

- [1] D. Enskog, Kungl. Svenska Vetenskaps Akad. Handl. **63**, 1 (1922).
- [2] L. de Sobrino, Can. J. Phys. **45**, 363 (1967).
- [3] M. Grmela, J. Stat. Phys. **3**, 347 (1971).
- [4] H. van Beijeren and M. H. Ernst, Physica **68**, 437 (1973).
- [5] J. Karkheck and G. Stell, J. Chem. Phys. **75**, 1475 (1981).
- [6] G. Stell, J. Karkheck, and H. van Beijeren, J. Chem. Phys. **79**, 3166 (1983).
- [7] M. Grmela and L. S. Garcia-Colin, Phys. Rev. A **22**, 1295 (1980).
- [8] M. Grmela and L. S. Garcia-Colin, Phys. Rev. A **22**, 1305 (1980).
- [9] M. Grmela, Can. J. Phys. **59**, 698 (1981).
- [10] E. S. Benilov and M. S. Benilov, Phys. Rev. E **97**, 062115 (2018).
- [11] E. S. Benilov and M. S. Benilov, Arxiv.org (2018), 1811.04709.
- [12] E. S. Benilov and M. S. Benilov, Phys. Rev. E **93**, 032148 (2016).
- [13] E. S. Benilov and M. S. Benilov, Phys. Rev. E **96**, 042125 (2017).
- [14] C. Tegeler, R. Span, and W. Wagner, J. Phys. Chem. Ref. Data **28**, 779 (1999).
- [15] T. R. Kirkpatrick, J. Stat. Phys. **57**, 483 (1989).
- [16] T. R. Kirkpatrick, S. P. Das, M. H. Ernst, and J. Piatecki, J. Chem. Phys. **92**, 3768 (1990).